University of Veterinary Medicine Budapest
Department and Clinic of Surgery and Ophthalmology

Comparison of radiographic liver volume and the 3D volumetry data based on CT examination in canine patients

By
Kim Kristina Wambsganß

Supervisor:
Dr. Attila Arany-Tóth

Budapest, Hungary
2017

Table of contents

List of Abbreviations

ROI	Region of Interest
DICOM	Digital Imaging and Communications in Medicine
CT	Computed Tomography
MRI	Magnetic Resonance Imaging
LDLT	Living Donor Liver Transplantation
CTV	Computed Tomography Volumetry
TLV	Total Liver Volume
BSA	Body Surface Area

1. Introduction

The liver is one of the most important organs in the body. Due to its essential function with regards to metabolism, digestion, immunocompetence, and the storage of nutrients within the body, it is considered a vital organ. In dogs, the liver weight equates to about three to four percent of the entire body weight (König and Liebich, 2011). The physiological liver parameters (size, volume, and weight) depend on various factors such as the breed, thoracic conformation and body weight of the dog. Liver volume is one of the most important clinical values and confers a degree of diagnostic significance. The hepatic volume is highly linked to the function of the liver. An alteration in liver size can indicate liver disease (Carlson, 1976), and/or other dysfunctions affecting the body, such as hepatic cirrhosis, hepatomegaly as a result of hepatic congestion, inflammatory and infiltrative disease or hepatic neoplasia. Therefore, obtaining a measurement of the exact liver volume may be considered to be highly beneficial for the diagnosis of certain medical conditions, to reduce present symptoms and limit further disease progression. Assessment of liver volume can also be useful in pre-operative patient evaluation. Taking the patients liver volume into consideration can minimize certain risks before further interventions. Many attempts have been made, through medical research, to determine the hepatic volume and accurately portray and describe the liver in its appearance. This has been proven to be especially difficult, primarily due to the livers anatomical complexity; its borders are indistinct with irregular shape (Douglas and Williamson, 1970). Previous attempts employed radiographic diagnostic assessment, computed tomography (CT) examination or software utilizing 3D reconstructions of the liver. This array of non-invasive techniques can be distinguished in their application, reproducibility, technique of measurement, expenditure of time, degree of difficulty, accuracy, and source of error. Three-dimensional evaluation of the liver volume using model reconstructions can be more precise and therefore beneficial in comparison to two-dimensional evaluation through conventional radiographic imaging. As a prerequisite for effective technique implementation, the segmentation process of 3D model reconstruction plays an essential role, however it has a high variability in its executional success.

Available software applications with further 3D volume reconstruction and visualization are not intended for clinical use and are currently solely utilized for research purposes (Strakos et al., 2015). Exact determination of the physiological liver volume is difficult due

to numerous variations in the natural ranges, making the mark between physiological and pathological volume difficult to define (Ackerman and Silverman, 1977).

2. Literature Review

2.1. Radiographic Anatomy of the Liver

The liver is situated primarily in the intrathoracic portion of the abdominal cavity. Partington and Biller, in their 1995 review paper, described the radiolucent line of the lung and diaphragm as a delineation of the cranial border of the liver. With lateral and ventrodorsal radiographic images of the cranial abdomen, an appraisal of liver size, shape, position, margination and opacity is possible. The caudal border is marked by the stomach, cranial duodenal flexure and the right kidney. The left lateral and right medial lobes protrude beyond the rib cage ventrally to form a triangular shape. This edge is surrounded by falciform fat. The left medial, right medial, and quadrate lobes are encircled by the dome of the diaphragm. The crus dextrum and sinistrum of the diaphragm outline the left and right lateral lobes. The cranial point of the right kidney indicates the caudal border of the caudate lobe. The gallbladder is situated between the right medial lobe and the quadrate lobe. The radiopacity of the gallbladder is equal to the livers parenchymal mass.

With a ventrodorsal projection, the costophrenic angle of the diaphragm and the fundus of the stomach are bound to the left lateral lobe of the liver. The left medial lobe is located craniomedially to the left lateral lobe and adjacent to the caudate and quadrate lobe. The caudate lobe lies more caudodorsally and the quadrate lobe is situated more cranioventrally in the abdominal cavity. With a ventrodorsal radiographic view, the right medial lobe together with the right lateral and caudate lobes, form the right caudal border of the liver which is demarcated by the duodenum and right kidney (Partington and Biller, 1995).

With a lateral radiographic view, the caudal boundary of the liver can be divided into three portions. Dorsally the liver margins are indicated by the cranial pole of the right kidney, in the central portion by the cranial part of the stomach and ventrally by the left lateral liver lobe. The location of the cranial pole of the right kidney indicates the caudal border of the right medial, quadrate and left medial lobes. The caudal border of the right lateral lobe and/or caudate lobe is depicted by the cranial duodenal flexure (Suter, 1982). As presented radiographically, the caudoventral tip of the liver appears as a wedge-shaped shadow and is

partially merged with the right medial and left lateral lobes (O´Brien, 1978). The lateral radiographic view is recommended for an estimation of the caudoventral tip (Root, 1974). The liver is observed as larger in right lateral recumbency than in left lateral recumbency (Grandage, 1974). Due to the anatomical structure of the liver, the caudate lobe is mainly situated on the right side of the abdomen and thus a better demarcation is made in right lateral recumbency (Lee and Leowijuk, 1982). In right lateral recumbency the left lateral liver lobe moves caudally and therefore produces a larger shadow than in left lateral recumbency (Kealy, 1979). The liver is connected through numerous direct and indirect ligamentous fixations to the proximal duodenum, right kidney and transverse colon (Cockett, 1986).

2.2. Radiographic Assessment of Liver Size and Volume

In a study by Van Bree et al. (1989), the real liver volume of 65 dogs was determined with water displacement. The results lay between 100 and 1105 ml. The radiographic liver length, as a measurement made with a lateral projection, defined as the distance between the most cranial part of the diaphragm to the apex of the liver tip, was statistically significant with real liver volume ($P < 0{,}000001$). The calculated liver length of the 65 dogs varied between 5,5 and 20 cm. They also noted, importantly, that the radiographic liver length was not a function of thoracic conformation and thus liver length seems to be a consistently reliable measurement, independent from thoracic conformation. A comparison between liver length and the eleventh thoracic vertebral body was made, which resulted in a correlation with liver volume/body weight ($P < 0{,}000001$). Furthermore, a correlation between the formula: liver length x thoracic depth x thoracic width, and real liver volume, was also statistically significant ($P < 0{,}000001$) (Van Bree et al., 1989).

Godshalk et al. stated in their 1990 review, that abdominal width, as the distance between the costophrenic recesses, and measured on a ventrodorsal radiograph, was statistically significant with liver volume ($r = 0{,}63$; $p < 0{,}05$). A line from the cranioventral border of the T11 body through the caudoventral border of the L4 body was drawn. A vertical line from the body of the third to last sternebrae was connected through the first line. This was defined as the abdominal height. Abdominal height, as a measurement using the right lateral view, was statistically significant with liver volume ($r = 0{,}78$; $p < 0{,}05$) (Godshalk et al., 1990).

In study published in 1987, Van Bree and Sackx surmised that the contours of the ventral

and caudoventral borders of the liver shadow could not be precisely identified and a superimposition of the silhouettes of both the liver and spleen occur frequently which makes the delineation of the caudal border of the liver shadow unachievable, thus having a significant impact on the liver measurements. It has to be mentioned that accurate results could be determined in only 14 of the 27 dogs that were enrolled in the study. In the left lateral radiographic view the liver shadow was more clearly delineated and less superimposition of the liver and spleen was perceived. This is, however, in contradiction to a statement of an earlier study which states that the liver shadow is more easily recognized in the right lateral radiographic view (Lee and Leowijuk, 1982). In approaching analysis of radiographic liver size, the side of recumbency should always be taken into consideration (Grandage, 1974). The liver quite often appears larger in right lateral recumbency than in left lateral recumbency (Van Bree and Sackx, 1987). The caudoventral tip of the liver has a more acute appearance in a right lateral radiographic projection than in a left lateral image (Lee and Leowijuk, 1982).

Moderate changes in liver size are difficult to determine. Gross liver changes, as depicted on a radiograph, are characterised by an enlarged hepatic shadow and rounding of the caudal hepatic margin, associated with an expansion of the caudoventral part of the liver behind the costal arch. Consequently, the stomach, right kidney, cranial duodenal flexure, and transverse colon are forced into a more caudal position in the abdominal cavity. Extreme enlargement of the liver can press the diaphragm more cranially into the thorax (Partington and Biller, 1995). Since many factors are involved in the presentation of the liver silhouette, the determination of a slight hepatomegaly should be done with care (Douglas and Williamson, 1970).

Microhepatica decreases the space between the diaphragm and stomach and will result in a cranial shift of the pylorus and a shift in the vertical stomach axis in relation to the tenth intercostal space (Partington and Biller, 1995). A false diagnosis of small liver may occur in deep-chested dogs (Doberman Pinscher), as the liver is positioned more vertically and within the costal arch (Partington and Biller, 1995). Furthermore, the cranial duodenal flexure, right kidney, and transverse colon are displaced cranially through decreased liver size, and a particularly full stomach can lead to a misdiagnosis of a small liver as the stomach may obscure parts of the liver (Partington and Biller, 1995).

In large, obese, older dogs, the liver shifts caudoventrally due to distended suspensory

ligaments, which may result in a false perception of liver enlargement (Partington and Biller, 1995). The visibility of the liver borders is influenced by the fat content of the falciform ligament (Gibbs, 1981). The falciform fat in obese animals elevates the liver in a dorsal direction and surrounds it with fat (Cockett, 1986). Young dogs have a more convex diaphragm (Grandage, 1974) and also a higher ratio of liver weight to body weight. In young dogs, the liver comprises 40 to 50 g/kg body weight, which decreases in older dogs to a ratio of 20 g/kg (O´Brien, 1978).

Variations between breeds occur and will have an impact on hepatic shape (Gibbs, 1981). The caudoventral tip of the liver is located more within the costal arch in dogs with a deep thorax and therefore with a steeper diaphragmatic slope. In narrow, deep-chested dogs the ventral lobes look small and upright in contrast to dogs with a shallow, wide thorax in which the liver tip protrudes caudally behind the costal arch to a greater extent and the ventral lobes appear thicker (Gibbs, 1981).

In their review, Van Bree and Sackx (1987) measured that in almost half of the deep chested dogs in their study, the liver tip, emerging behind the curve of the last rib, was greater than one times the length of the eleventh thoracic vertebral body. This finding lies in contradiction to a wealth of other literature which states that in dogs with a deep chested thorax, the caudoventral tip of the liver is located within the costal arch (Gibbs, 1981). Even though dogs may possess the same deep-chested thoracic conformation, a boundless range in liver size results in a difficulty in diagnosing hepatomegaly (Van Bree and Sackx, 1987).

Choi et al. (2012) compared the radiographic liver size measurements obtained from brachycephalic Pekingese dogs, non-Pekingese brachycephalic dogs, mesococephalic dogs and Pekingese which harboured a liver disease. Parameters such as body weight, liver length, eleventh thoracic vertebral length, thoracic depth and width were assessed on ventrodorsal and right lateral abdominal radiographs. The liver length is defined as the distance from the ventral border of caudal vena cava to the apex of the hepatic caudal border. The depth of the thoracic cavity was defined by drawing a line between the ventral border of the fourth lumbar vertebra (L4) and the ventral border of the eleventh thoracic vertebra (T11) to the upright axis from the caudal tip of the sixth sternebra. For the measurement of the thoracic width, the distance between the right and left costophrenic

recesses was calculated. The liver volume was calculated as a ratio of liver length/eleventh thoracic vertebral length and liver volume/body weight. Pekingese dogs without liver disease had a smaller liver volume/body weight and liver length/T11 vertebral length proportion than non-Pekingese brachycephalic and non-brachycephalic breeds. Liver volume/body weight and liver length/T11 vertebral length ratios were higher in Pekingese with liver disease than in any of the dogs from the other groups. Based on the discovery that the liver of brachycephalic Pekingese dogs is smaller than the liver of other breeds, Choi et al. proposed a calculation of the liver length with the multiplication factor of 4,64 times the length of the eleventh vertebral body. This ratio was significantly smaller than in non-Pekingese brachycephalic breeds (5,16 times). In non-brachycephalic breeds the length of the liver can therefore be calculated as 5,4 times of the length of the eleventh thoracic vertebral body (Choi et al., 2012).

The respiratory phase also has an influence on the liver location, as during inspiration the liver shifts caudally, while expiration moves the liver in a cranial direction (Van Bree et al., 1989). Therefore, during inspiration the liver tip further exceeds the costal arch. According to the type of respiration, the liver can move up to a centimetre in a cranial or caudal direction (Grandage, 1974). The end of the expiration phase has been determined as the optimal time for image capture to enhance organ separation and minimize motion artefacts in radiographic imaging (Partington and Biller, 1995).

For a better visualisation of the caudal margin of the liver and its separation from the stomach, 1 ml/kg of liquid barium sulphate is given orally (Partington and Biller, 1995). To prevent superimposition of the bowel and tissue compression of the organs, it is recommended that the patient fasts for 18 to 24 hours before the procedure commences, and 4 hours before the investigation an enema is given (Partington and Biller, 1995). Focal liver alterations such like cysts or abscesses are better assessed ultrasonographically (Partington and Biller, 1995).

2.3. Comparison of Body Variables with Liver Volume

Vauthey et al. (2002) determined a formula predicting total liver volume (TLV) based upon the body surface area (BSA) in 292 clinically normal human adults. A multicenter study was completed to assure that reliable results were obtained from a variety of equipment

and software, as each study utilized a different method for the 3D reconstruction of the liver. A linear regression formula for the TLV, based on BSA, was determined. The results showed a high correlation ($p < 0,0001$) between TLV and BSA, with a 95% confidence interval and 95% predictive interval (Vauthey et al., 2002).

In their review, Godshalk et al. (1990) studied 16 dogs and measured their liver volume and weight by water displacement following euthanasia. The volume was further compared with body and liver variables. The body surface area was calculated with the following equation: Body surface area= [(4×body weight)+ 7] /(body weight+90), where body weight was expressed in kilograms and the body surface area in meters squared. With a correlation coefficient of $r = 0,93$, the body surface area was statistically significantly correlated with liver volume ($p < 0,0001$). In a comparison between several body variables and liver weight/volume, the body weight had the highest correlation with liver weight ($p < 0,001$; $r = 0,95$). The correlation coefficient ($p < 0,001$; $r = 0,94$) between body weight and liver volume was statistically significant. However, a comparison between the gender and the liver volume was not significant ($p < 0,001$; $r = 0,17$) (Godshalk et al., 1990).

2.4. 3D Slicer and Other Image-Based Volumetry Methods

3D Slicer is a free, open source software package for image processing and scientific visualization for physicians, academics, and the general public. It was constructed by the National Institute of Health and a worldwide developer community. It is available on multiple operating systems, namely Windows, Linux and Mac OSX. 3D Slicer is intended for research purposes and has not been validated for clinical use. More than one-hundred modules exist within the Slicer, including segmentation, image editing and volume rendering which function as useful, widely applicable features of this software. 3D Slicer is also frequently used to prepare data for 3D printing. When choosing a module, the left part of the Slicers interface changes, revealing a variety of features and tools which exist for that particular module. The right part of the Slicers interface is for visualizing the imaging data. The interface is strongly user dependent but it can be organised in classical 3D, transverse, sagittal and coronal views. The 3D Slicer supports the reading of the DICOM CT database, for example, as well as an assortment of other formats.

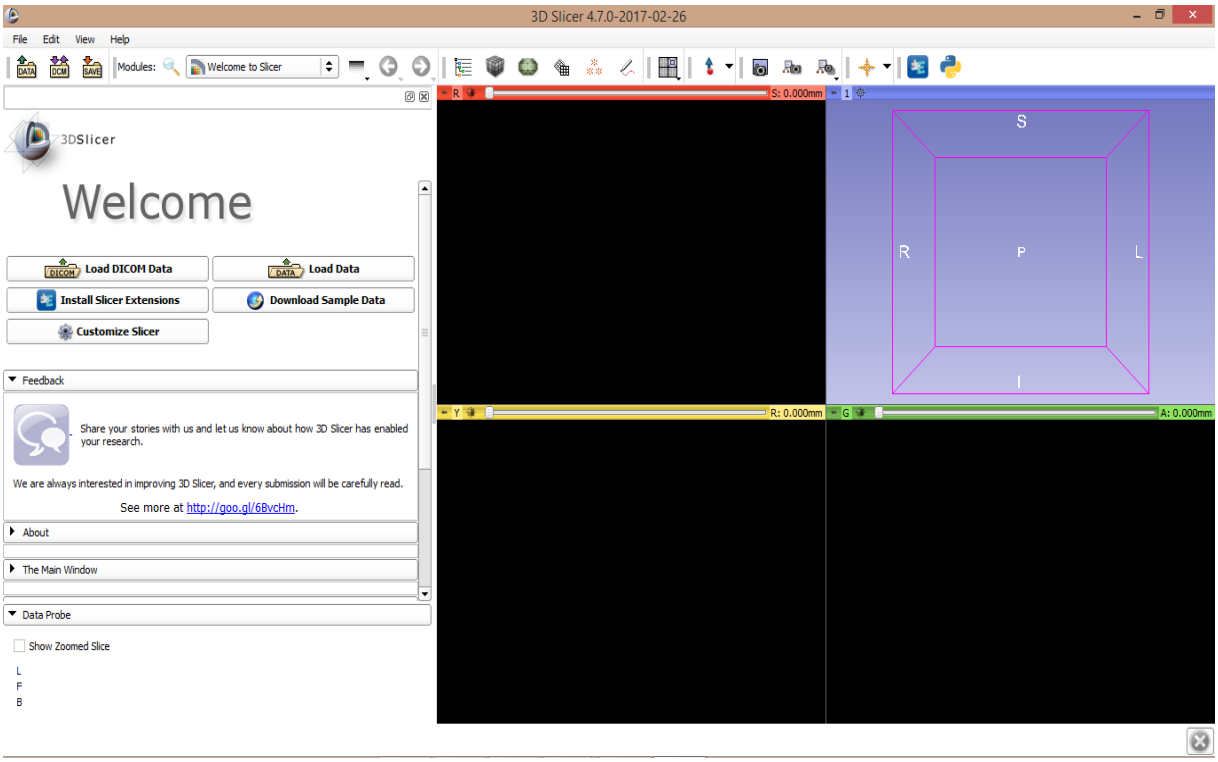

Figure 1. The typical Graphic User Interface (GUI) of Slicer 4.7.0 nightly version with the slice viewer (red, yellow and green slice), 3D viewer and the toolbar above.

With the help of the segmentation module, 3D Slicer is able to isolate a specific region of interest, thus offering further 3D remodelling of organs and tissues (http://slicer.org). Successful manual image segmentation requires training and is highly time consuming. Every application form requires an immense data source to achieve a precise representation of the region of interest. Due to this fact, the scan spacing intervals should be kept small with the contiguous slices not exceeding a thickness of 3 mm (Strakos et al., 2015). In their review, Strakos et al. focused on available software solutions which offer image segmentation of the liver with further 3D model reconstruction. Five applications, which are either open-source or free software solutions, were selected:

- Itk-Snap
- GeoS
- Lisa
- Osirix
- 3D Slicer

3D model reconstruction with further volumetric model reconstruction of different body parts or whole organs can be very beneficial in medical imaging, especially for diagnostic medicine. Through a timelier and more precise diagnosis of a disease, an operation can be

better planned, thus reducing the associated risks of the intervention. The segmentation can be used to isolate a particular region, which can then be utilized for further 3D model reconstruction. The level of difficulty varies from bones, which are very easy to segment, up to the liver, which is one of the most challenging organs to segment. Segmentation methods can be divided into automatic, semi-automatic and manual processes. To make a reliable comparison between these five applications, a reference volume (VR) was evaluated using manual segmentation with the help of 3D Slicer. The reference volume in this study is 137,024 ml. The segmented volume (VS) was then obtained from all 5 available software with semi-automatic segmentation. Furthermore, a relative volume difference (RVD) was calculated and used for comparison, stated in percentage. The relative volume difference was calculated with the following equation:

$$\mathrm{RVD}=100*\frac{(\mathrm{VS}\text{-}\mathrm{VR})}{\mathrm{VR}}$$

With a semi-automatic image segmentation volume of 130,290 ml, the 3D Slicer was closest in accuracy with that of 3D model manual segmentation. The relative volume difference was -4,915%. The least accurate result was observed using GeoS which was not able to create a complete 3D model, thus this software failed. The second-best result in semi-automatic segmentation was observed with Lisa, with a segmented volume of 127,910 ml and a relative volume difference of -6,651%. The finest transitions between the segmented slices were performed by Osirix due to the application of polygon regions of interest for segmentation. However, it should be noted that Osirix has the second poorest result, with a segmented volume of 101,444 ml (Strakos et al., 2015).

In their review, Lim et al. (2014) state that imaging-based volumetry has become increasingly important in current clinical practice. Liver volume estimation is a key parameter for successful hepatic resection and living donor liver transplantation (LDLT) (Guglielmi et al., 2012). The selection criteria for an appropriate individual for LDLT is an important procedure as the liver of the donor must be adjusted to the liver of the recipient in size to ensure the safety of both the donor and recipient. The size of the donor´s liver influences the postoperative success of the liver graft procedure (Ben-Hain et al., 2001). A successful liver graft procedure is influenced by graft size and by pre-existing disease in the donor´s liver. Preoperative imaging is required to eliminate any possibility of liver cirrhosis, steatosis, and malignant neoplasms in the donor´s liver. Analysis of the recipient’s disease state prior to surgical intervention is essential due to the fact that present

malignancies have a tendency to rapidly progress. It is also imperative to perform a postoperative assessment of liver size, to ensure graft regeneration of the liver tissue (Tsang et al., 2008).

In their review, Lim et al. (2014) state that imaging-based volumetry, with emphasis on CT, has been widely used to capture and visualise the liver in its entirety. Contrast-enhanced CT provides a better delineation of the vascular anatomy of the liver and the outline of a hepatic tumor is more easily recognised with contrast CT than without. Other liver imaging methods, such as MRI and ultrasound, have also exhibited reliable organ volume measurements. MRI images have a higher contrast within the soft tissue but it is a more expensive diagnostic method than CT. The different methods of CT volumetry (CTV) can be divided into three categories: manual, semi-automated and automated. The traditional method of analysis is based on manual contour tracing of the liver with further summation of each transverse section. Such manual calculations are highly user dependent and time consuming. The segmentation can be done with a standard optical mouse or with a freehand electromagnetic pen tablet. In their precision, these two methods are comparable, but the required mean segmentation time was remarkably shorter with the freehand electromagnetic pen contour method. In order to decrease the time needed for segmentation and to minimise the effort of the operators, automated and semi-automated approaches of volumetric reconstruction of the liver have been proposed (Lim et al., 2014).

Complex techniques and algorithms have been constructed to find automated methods of volumetry. Active contour segmentation is widely used for automatic image segmentation and is based upon finding the contour of an object by forming a rope around its boundary. However, in many cases automatic segmentation is unsuccessful. This is due to the fact that often the edge is not continuous due to comparable intensity of an adjacent organ or the CT images have a low contrast quality (Lim et al., 2014). Automatic segmentation methods do not allow the operator to intervene, and therefore a correction of error is not possible, leaving no room for refinement. The semi-automated segmentation method provides more control over the volumetric result as the user is able to influence the segmentation process itself. During this method, the user sets, for example, live wire or boundary points around the object to be segmented. In the 2014 study by Lim et al., the average expenditure of time for automated volumetry is around 0,57 ± 0,006 min/case. The user time required with a manual segmentation method is 39,4 ± 5,5 min/case, whereas

semi-automated segmentation takes 27,3 ± 4,6 min/case (Lim et al., 2014).

Software solutions for the calculation of liver volume, such as OsiriX, have been found to have a positive correlation with conventional CTV. Furthermore, the image section thickness can influence the result of the liver volume. Since an accurate liver volume is based on precise segmentation, one might assume that the smaller section thickness the more accurate the result. However, the calculated volume significantly increases as the slice thickness decreases. Thus, there is an inverse correlation between the slice thickness and the liver volume (Lim et al., 2014).

3. Hypothesis and Aims

The liver volume is an extremely useful indicator of a dog's health status. In the last decade, the implementation of computer technology has changed the processing and visualization of medical image data from conventional radiographs to CT generated images. Data technology offers a three-dimensional visualization of a CT image data set, which is subsequently used in the planning and execution of surgical procedures. This study aims to compare 3D volumetry data, acquired through the use of the 3D Slicer software, with several radiographic parameters obtained from lateral and ventrodorsal projections and numerous body measurement variables.

It has been stated that radiography is an unreliable method for liver size estimation in small animals (Gelfand, 1975). Although a radiographic approach to liver size is generally discussed (O´ Brien, 1978), it still holds great importance in a clinical setting and it is often included in the radiologists' investigation. An objective assessment is only attainable if there are general, defined agreements as to what constitutes normal and abnormal presentations, together with a tolerable level of standard deviation (Cockett, 1986). A wide range of values makes it difficult to define any standard, and reflects a broad morphological variation within the breed (Cockett, 1986).

One of the prime focuses of this study was the application of the 3D Slicer as a useful software program for self-conducted research. The 3D Slicer is a continuously developing image-guided research package, which is frequently used to construct and visualize collections of CT data, such as DICOM files. The strengths and limitations of using 3D volumetry data based on CT examination with the help of 3D Slicer will be discussed in

this study. While using the 3D Slicer it should be clarified whether the volumetric computer-assisted measurements are reproducible and practicable in a clinical setting. The primary objective of this study is to analyse the 3D Slicer in its application and reproducibility, and to associate these results with the conventional radiographic volume assessment. We aim to explore whether there are certain correlations between liver and body parameters and the volume measured with the 3D Slicer.

4. Material and Methods

4.1. Case Studies

Altogether, 26 suitable dogs were admitted in to the study. Lateral and ventrodorsal abdominal radiographs and contiguous abdominal CT scans of 26 patients were viewed in order to find suitable candidates for the study. Their clinical history was available and radiographic images of patients with obvious liver abnormalities or deformities were noted and these patients were removed from the sample population. The breed and gender of the dogs were not taken into consideration in this study. These 26 dogs were also of various ages with diverse thoracic conformations. The body weight of the dogs varied from 2,5 to 56 kilograms and had an average age of 9,5 years. Radiographic and CT images were provided by the Department and Clinic of Surgery and Ophthalmology in the University of Veterinary Medicine in Budapest, Hungary.

The images were sourced through the DICOM database and focussed on the abdominal area. Single slice helical CT scanner (CT-e GE) was used. The slice thickness was 3 mm, with 3 mm intervals. The number of slices which underwent segmentation ranged from 70 to 90. Three-dimensional liver volumes were created by a summation of the livers two-dimensional section areas. The cross-sectional parts of the liver were segmented manually for each individual scan and volumes were then determined using 3D Slicer. Adjacent areas, such as the gallbladder and the intrahepatic caudal vena cava, were included in the volume determination process. Several parameters, including liver length, were calculated from the radiographs in order to compare and correlate with the determined liver volume. The age, body weight, and body surface area were also recorded and included in our analysis. The body surface area was calculated with the following equation:

$$\text{Body surface area} = [(4 \times \text{body weight}) + 7] \ / (\text{body weight} + 90)$$

4.2. Liver Volumetry with 3D Slicer

The obtained CT images were evaluated with 3D Slicer nightly version 4.7.0. The liver volume was analyzed with the following steps, under the guidance of Dr. Andras Lasso, a member of the worldwide developer Slicer community:

- Click on “Welcome to Slicer” and select “All Modules” to display the list of Slicer modules.

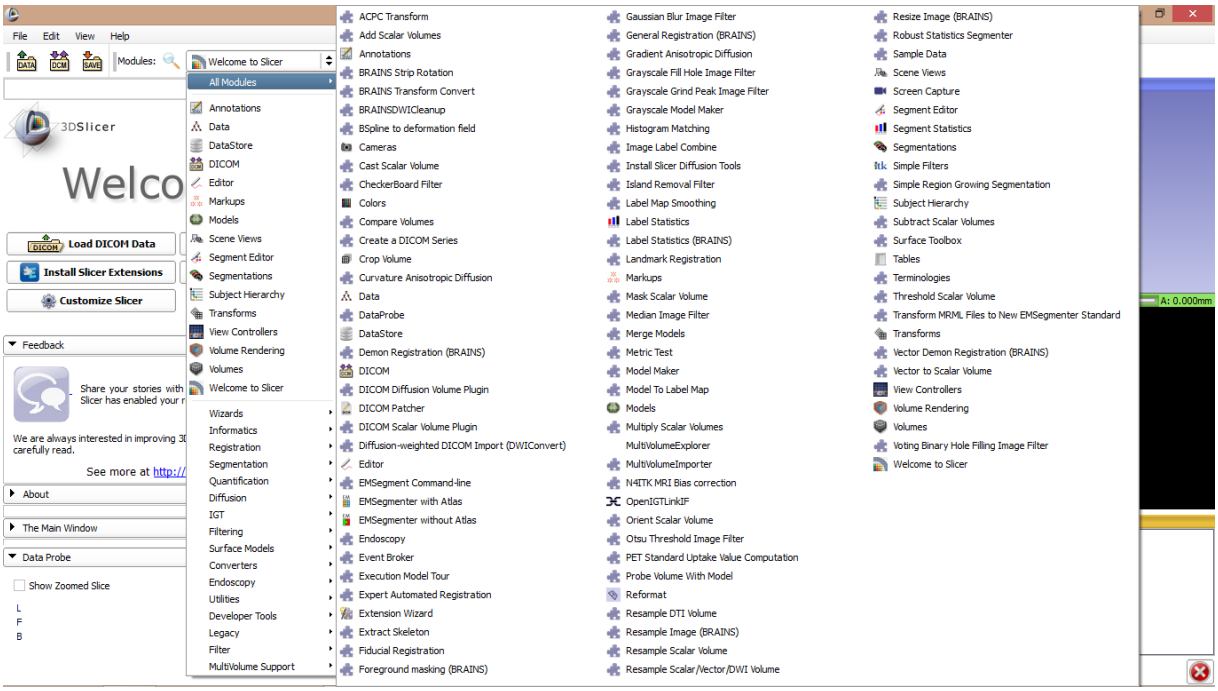

Figure 2. Slicer version 4.7.0 contains over 100 modules for cropping, segmentation and 3D visualization of medical image data.

- Loading the CT abdominal dataset with the DICOM module.
- The DICOM Browser appears and clicking on “Import” allows the selected file to be uploaded to the Slicer.
- A window indicates the completion of the “DICOM Directory Import”.
- The DICOM Browser specifies information regarding the patients name, identification number, birth date and time, sex and age.
- Select the desired dataset in the DICOM Browser and click “Load”.
- Slicer displays the axial, coronal and sagittal views of the abdominal dataset.

- Select the “Crop Volume” module and click on “Display ROI” to enable the cropping function. The aim is to crop the volume to the region where the organ of interest lies.
- A shrinking of ROI until it contains only the liver was done to specifically target the region which contained the volume of interest.
- Click on “Isotrophic Spacing” to make the voxel size more balanced.

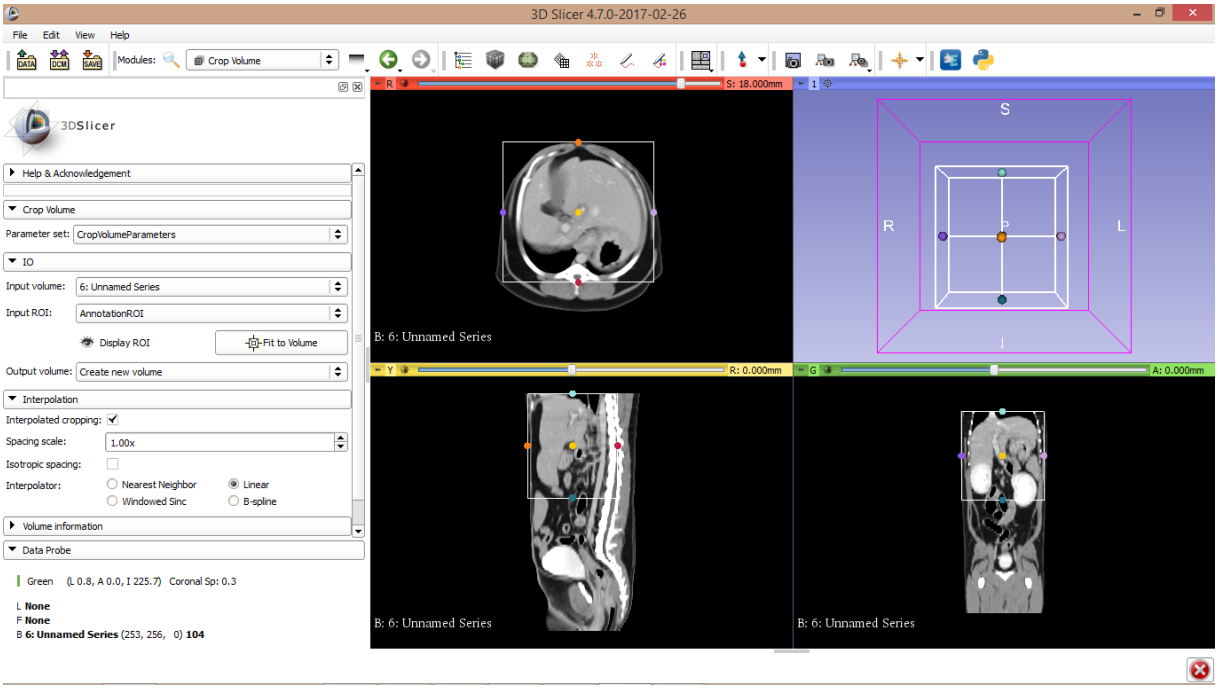

Figure 3. Slicer Interface with the Crop Volume module on the left side and a loaded liver data set on the right side in a four up view: axial slice (upper left window, red), sagittal slice (lower left window, yellow), and the coronal slice (lower right window, green). The Crop Volume module displays the ROI.

- Select the core module “**Segment Editor**”**.**
- Click on “Add Segment”.
- The brightness level can be changed under the core module “Volumes” by choosing “Window Level Editor Presets”. Alternatively, an underlying scale allows the brightness to be altered manually.
- The brightness can be adjusted through several scrolling options on the mouse. With a left click and drag, the contrast is adjustable, while a right click and drag allows a zoom in and out function.

- The threshold effect can ease in the recognition of the liver and it can mask other organs.
- Using the "**Draw Effect"** can trace the liver contours manually, slice by slice. Press "Enter" to fill the liver contour with a selected colour.

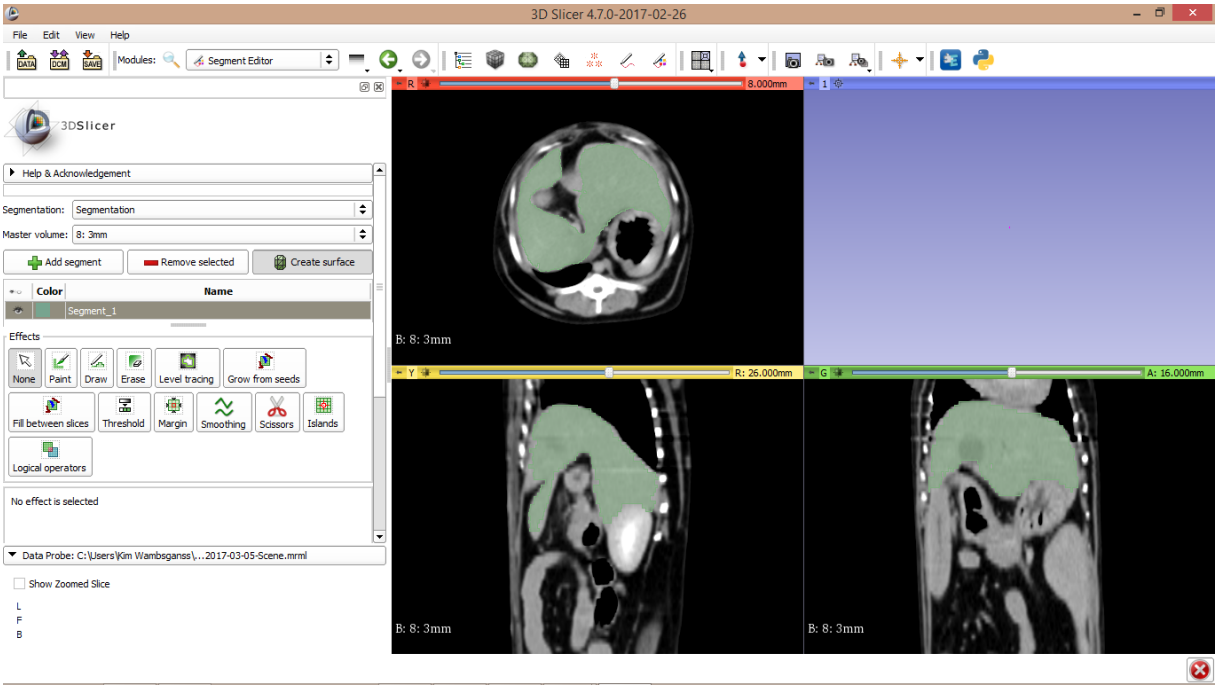

Figure 4. Segmented liver using the fill between slices effect. Segment Editor module.

- With the help of the "fill between slices effect", every 5th slice can be stained. The unprocessed slices are automatically filled.
- After filling between slices, a check through all the slices one by one is necessary to verify that the segmentation is correct and, if necessary, modifications may be performed.
- To make corrections the "Erase" effect is helpful to delete regions that did not contain the organ of interest or are not clear enough. The diameter of the "sphere-brush" is variable.
- It is also possible to make refinements with the "paint brush" after the edges have been drawn.
- A useful tool, for better orientation within the slices, is the crosshair from the toolbar. It shows where the cursor is in different views. While holding down the

shift key and moving the mouse, the “crosshair” can be placed at the region of interest. The corresponding slices for that area are then automatically shown.

- Click on “Initialize” and “Apply”.
- Click on “Create Surface” to build a 3D reconstruction of the segments.
- Choose the module “**Segment Statistics”** for the calculation of the liver volume of the volumetric model.
- Set the grayscale volume to 3mm cropped.
- Create a new table for the output and click “Apply”.
- The LM volume cc (Label Map volume) is indicated in cubic centimetres.
- The file can be easily saved in STL format, for example.

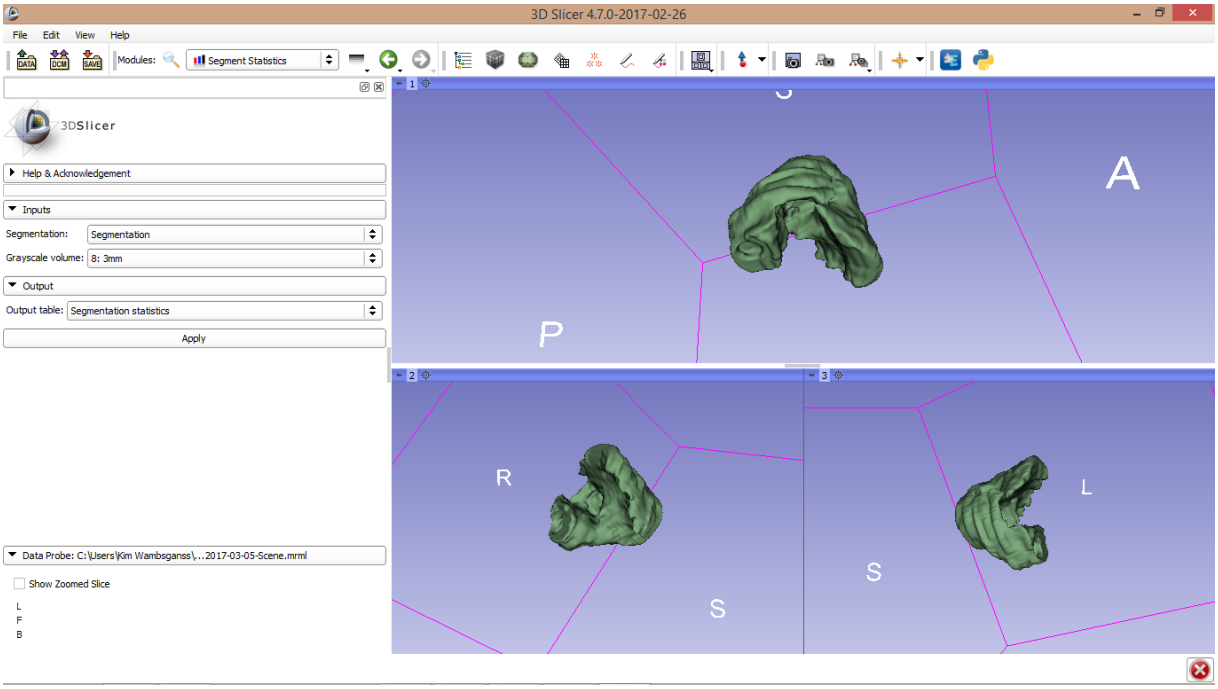

Figure 5. Triple 3D visualization of the liver. The Label Map volume in this patient is 136,645 cm³. Its body weight is 2,5 kilograms and the age is 13 years.

4.3. Evaluation of Radiographic Parameters

Measurements of the thoracic width with a ventrodorsal view, and liver length, liver area and thoracic depth on the lateral view, were made with 3D Slicer. For the evaluation of the radiographic liver area, lateral radiographs were taken for each patient. With the “drag and drop” function the images were placed into the sagittal slice of 3D Slicer. This is the yellow, lower left window of the 3D Slicer interface. To bring the radiographic image into a straight position, the “Reformat Module” was chosen and the rotation slider was

regulated. The radiographic image was reduced to demonstrate the liver, with the help of the “Crop Volume Module”. Switching to the core module “Segment Editor” allowed manual tracing of the lateral area of the liver. By pressing “enter”, the tracing is accepted and the borders are filled automatically by the software. With the “Create Surface” function, a 3D surface with a front face, back face, and a very thin rim was constructed. Under the module “Segment Statistics”, the liver area was calculated. To receive a 2D area, the reported value was divided by the factor 2. The area was expressed under the term CS surface (closed surface), and was indicated in mm².

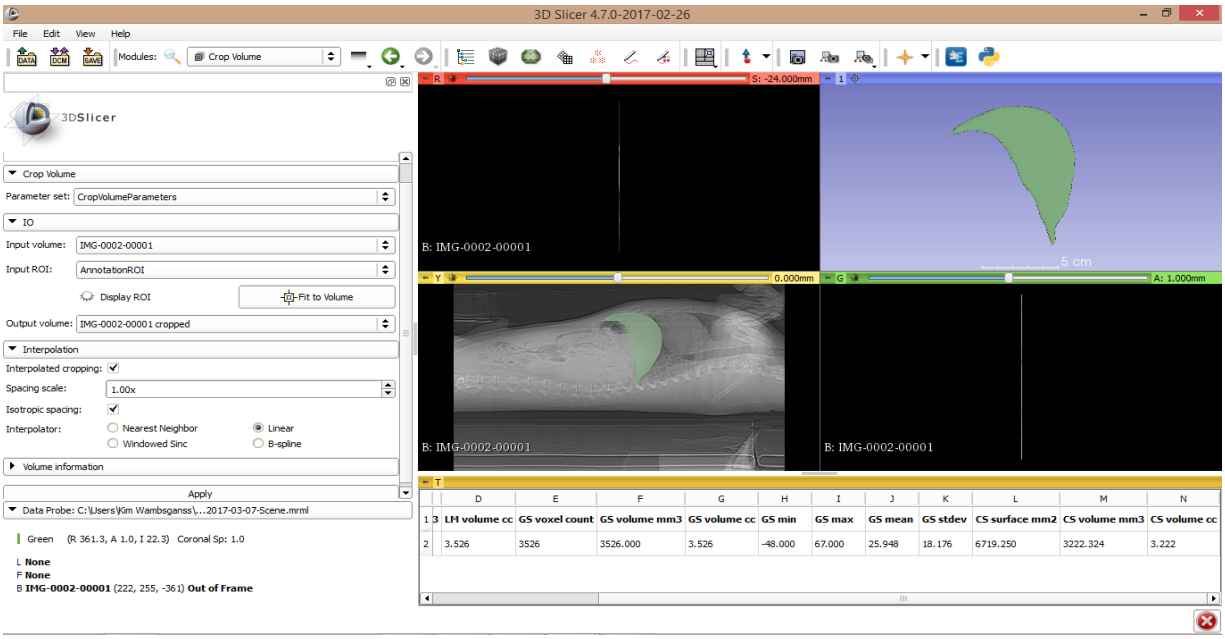

Figure 6. Liver area measurement with 3D Slicer 4.7.0 nightly version. The radiographic image is placed in the sagittal slice and the liver was segmented and furthermore the CS (closed surface) was calculated with the module Segment Statistics. In the 3D visualization slice the segmented liver is displayed. To receive a 2D area the reported value must be divided by the factor 2. (In this case the CS area is 6719,250 /2 =3359,625.

For the evaluation of radiographic liver length, two points were set on the lateral radiographs which were subsequently connected through a straight line with the “Ruler” from the Slicers toolbar. One point was set at the most cranial part of the diaphragm and the second one at the apex of the liver tip. These 2 points were then connected. The radiographic liver length was indicated in mm.

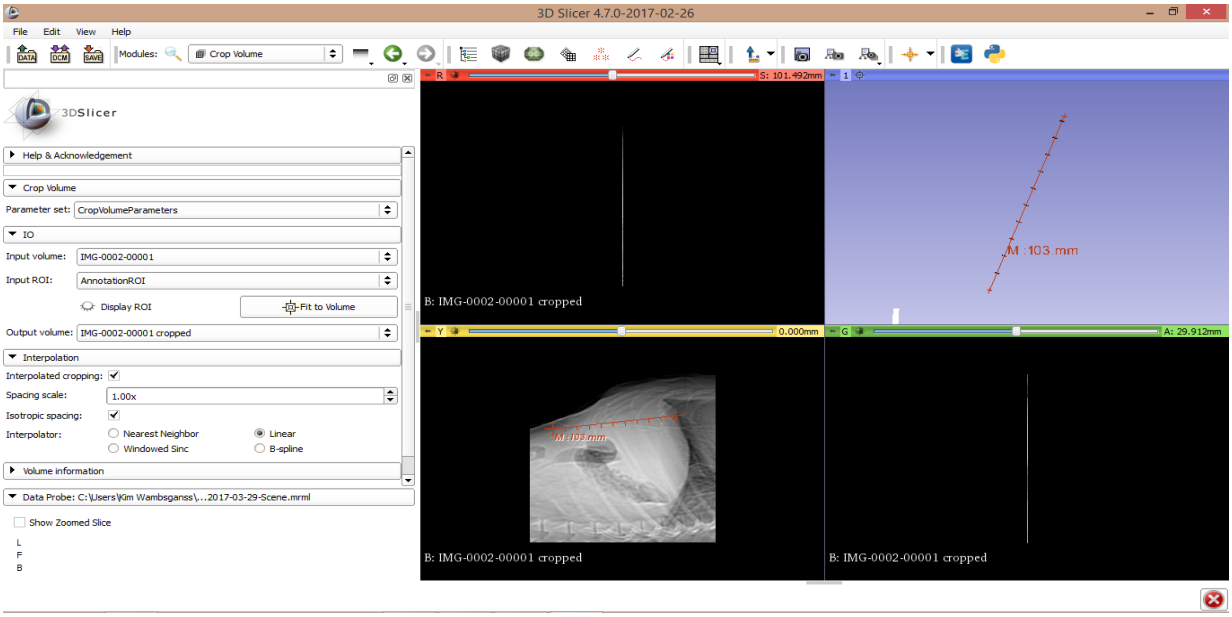

Figure 7. Liver length calculation with 3D Slicer 4.7.0 nightly version. With the Ruler, the distance from the most cranial part of the diaphragm to the apex of the liver tip was measured. The resulted length of the patient named Vackor is 103 mm. This dog has a body weight of 13,6 kilograms and is 5 years old.

The thoracic depth on the lateral radiograph was determined through drawing a line from the caudal tip of the sternum in a dorsal direction, perpendicular to the thoracic spine. The thoracic depth was indicated in mm. An assessment of the thoracic width was made by measuring the distance between the costophrenic recesses, indicated in mm.

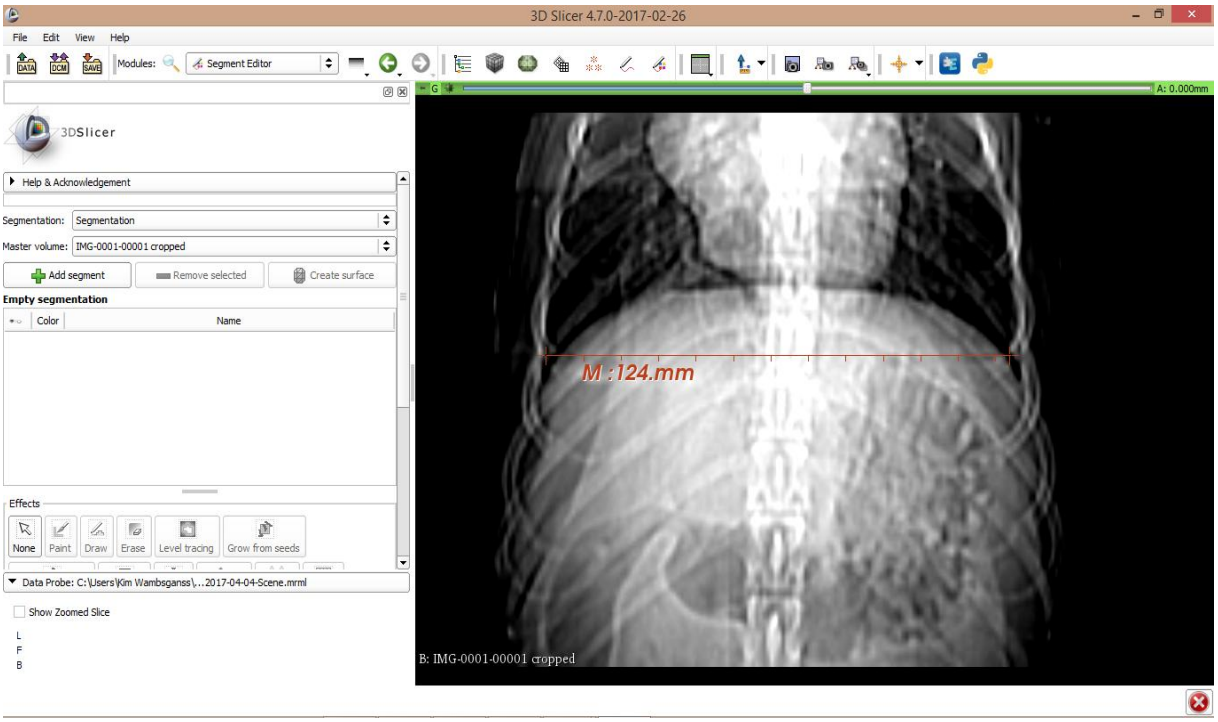

Figure 8. Measuring of the thoracic width by the distance between the costophrenic recesses. The ventrodorsal radiograph was used and inserted into the coronal slice of the 3D Slicer.

4.4. Statistical Analysis

The results of the measurements taken were analyzed with Microsoft Excel. For all the statistical analyses the level of significance was set to $P < 0.05$. P values < 0.1 were considered to be statistically significant. Results were expressed as Mean ± SEM.

Linear Regression and the Pearson Product Moment Correlation Coefficient R were computed in order to evaluate the correlation between the liver volume and several parameters obtained from radiographic analysis. In the scatterplot, the liver volume was set for the X-axis and the optional parameter was assigned for the Y-axis. Furthermore, a trend line was superimposed on the linear regression analysis scatterplot and a regression equation was determined. The liver volume, measured for all 26 dogs, was then compared with body weight, body surface area, age, and the following radiographic parameters:

I. Liver area (mm^2)

II. Liver length (mm)

III. Thoracic width (mm)

IV. Thoracic depth (mm)

V. LL × TD × TW (mm^3)

5. Results

The measured liver volume for the 26 dogs ranged between 136 cm^3 and 1196 cm^3 and radiographic liver length ranged between 46 and 127 mm. The average liver volume was 485,2 cm^3. All the parameters obtained from the radiographic images had a statistically significant correlation with liver volume ($p < 0,05$).

The highest correlation was between liver volume and body surface area ($r = 0,9473$). The correlation coefficient ($r = 0,7024$) between liver length, as the length of the axis from the most cranial part of the diaphragm to the apex of the liver tip, and liver volume was also statistically significant ($p < 0,0001$). Radiographic liver area, a measurement constructed from the lateral abdominal radiographs of all 26 subjects, closely correlated with liver volume ($r = 0,8910$; $p < 0,0001$). The thoracic width, as the distance between the costophrenic recesses on the ventrodorsal radiograph, was significantly correlated with liver volume ($r = 0,9212$; $p < 0,0001$). The correlation coefficient ($r = 0,8494$) between thoracic depth, as the line from the caudal tip of the sternum perpendicular to the thoracic spine, was statistically significant with liver volume ($p < 0,0001$).

The correlation coefficient ($r = 0,9291$) between the formula LL × TD × TW and the liver volume was statistically significant ($p < 0,0001$). The regression equation was $y = 0,0003\times + 42,118$, with y representing the liver volume and x representing LL × TD × TW. Based on this formula, a calculated volume was determined. The difference between the volume calculated from the LL × TD × TW by the equation and the initial volume was further calculated ($r = 0,2876$).

The correlation coefficient between the dogs age and the liver volume was not statistically significant ($r = 0,1100$; $p = 0,5932$). The subjects' body weights, averaging 20 kilograms,

was statistically significant with liver volume (r = 0,9436 ; p < 0,001). The calculated body surface area compared with the liver volume also showed a high correlation (r = 0,9473 ; p < 0,001).

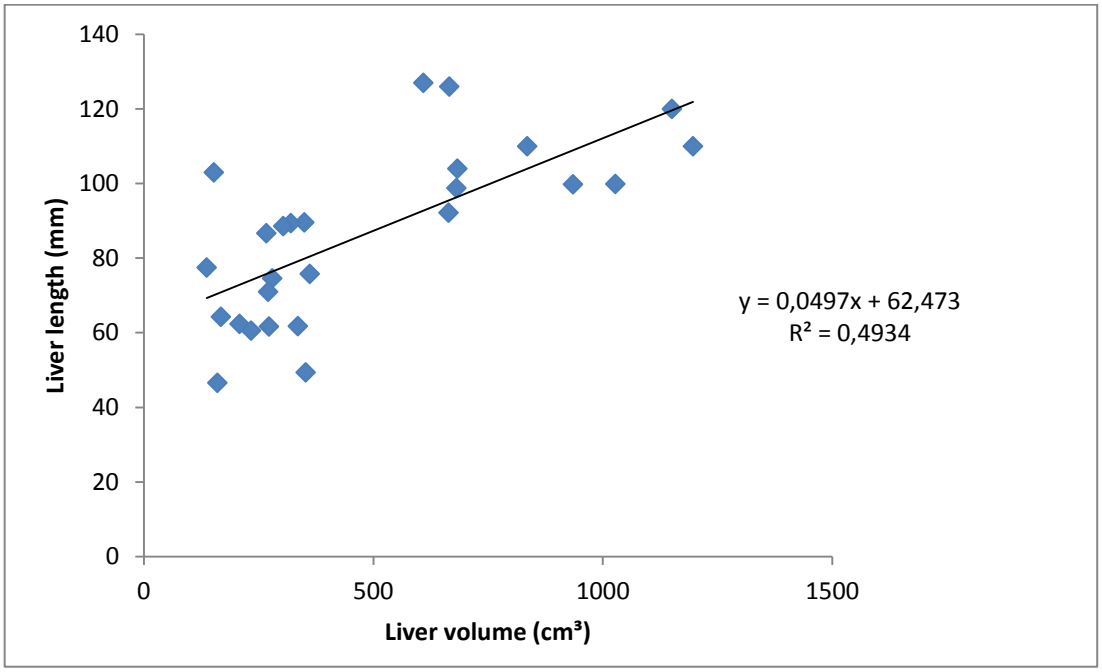

Figure 9. Scatter plot and regression line of the correlation between liver volume (x-axis) and liver length (y-axis). The correlation coefficient R^2 = 0,4934.

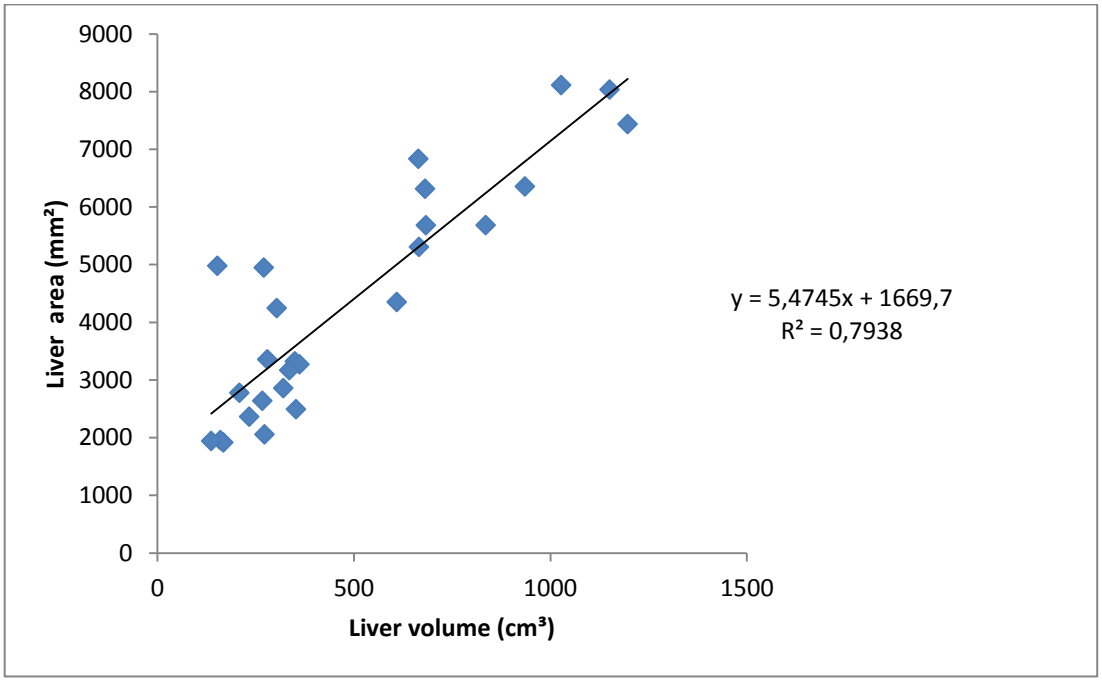

Figure 10. Correlation between liver volume (x-axis) and liver area (y-axis). The correlation coefficient R^2 = 0,7938.

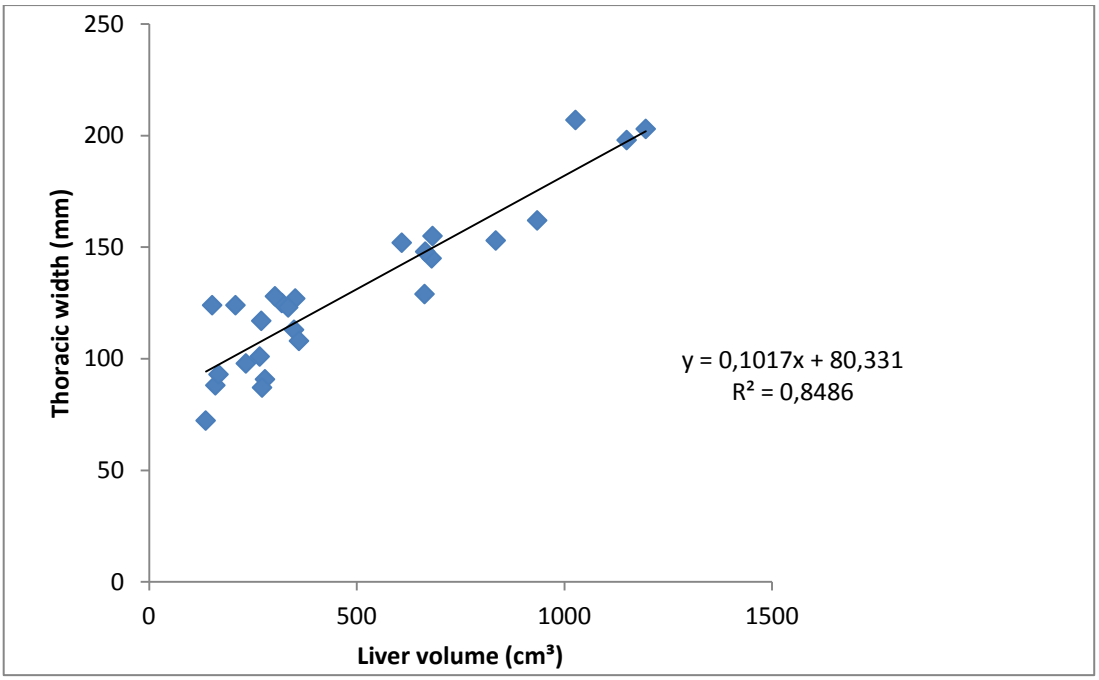

Figure 11. Correlation between liver volume (x-axis) and thoracic width (y-axis). The correlation coefficient R² = 0,8486.

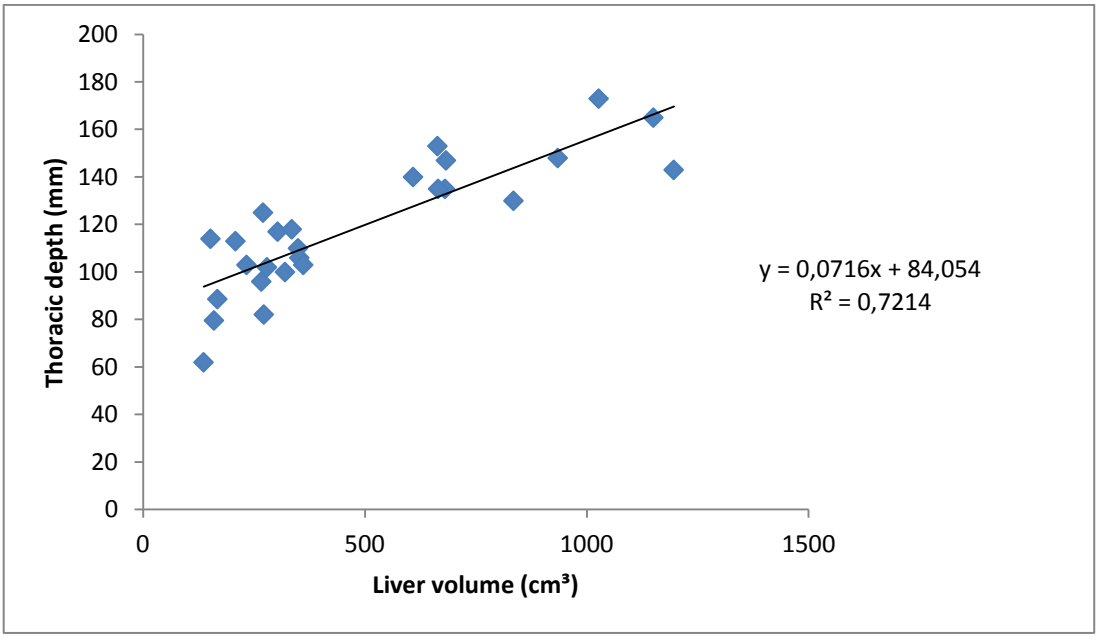

Figure 12. Correlation between liver volume (x-axis) and thoracic depth (y-axis). The correlation coefficient is R² = 0,7214.

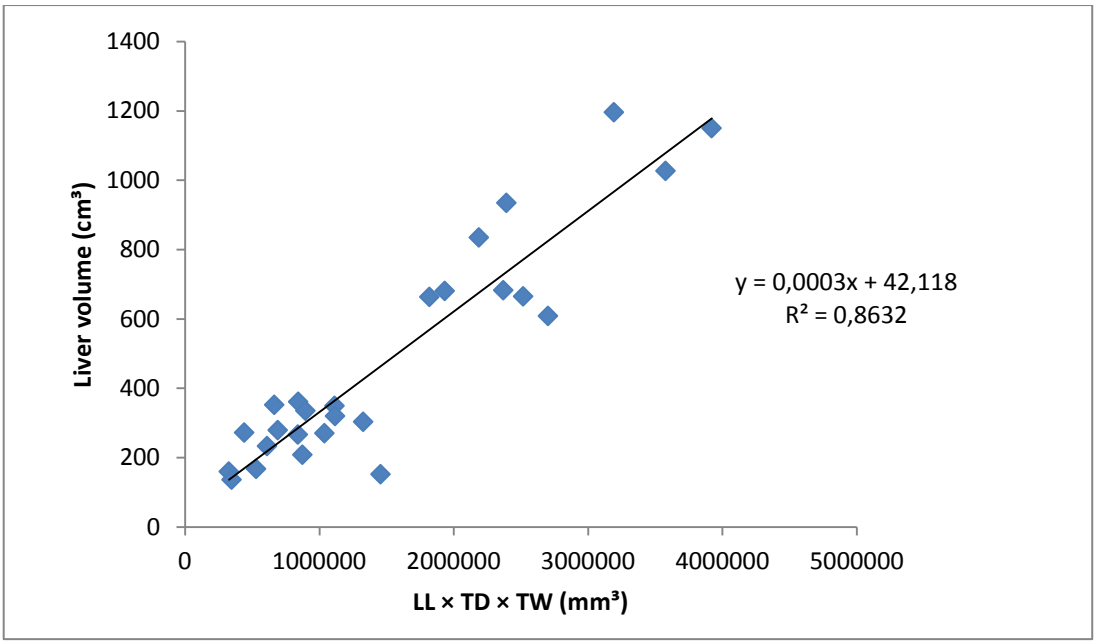

Figure 13. Correlation between the formula liver length × thoracic depth × thoracic width (LL × TD × TW) and liver volume. The correlation coefficient R^2 = 0,8632. The regression equation is y = 0,0003× + 42,118.

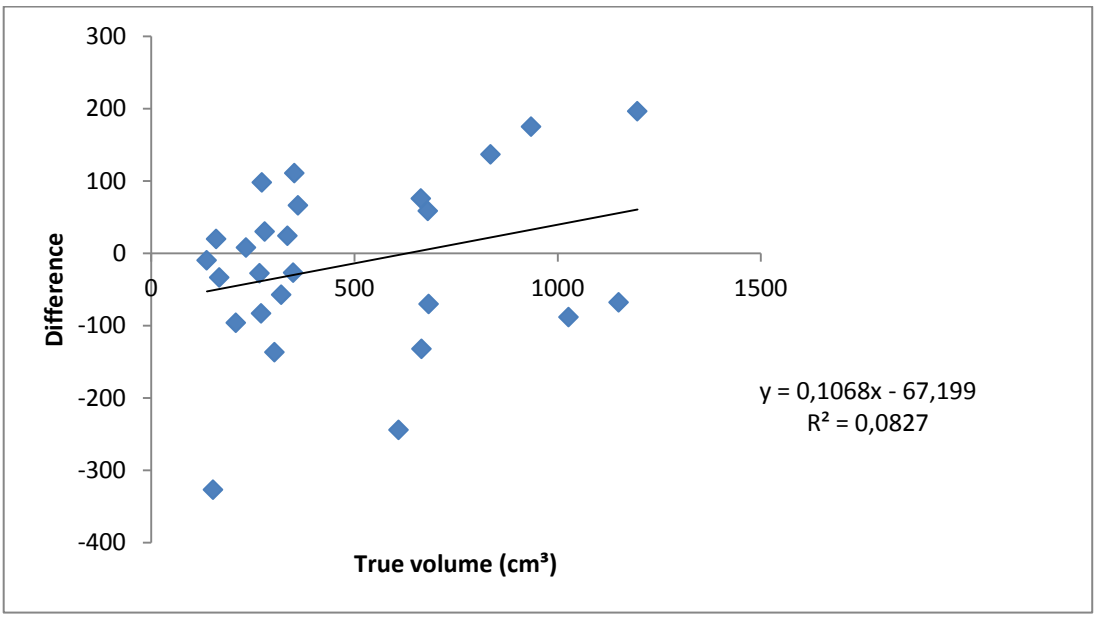

Figure 14. Correlation between the true volume (x-axis) and the difference between the volume calculated from the LL × TD × TW by the equation and true volume (y-axis).

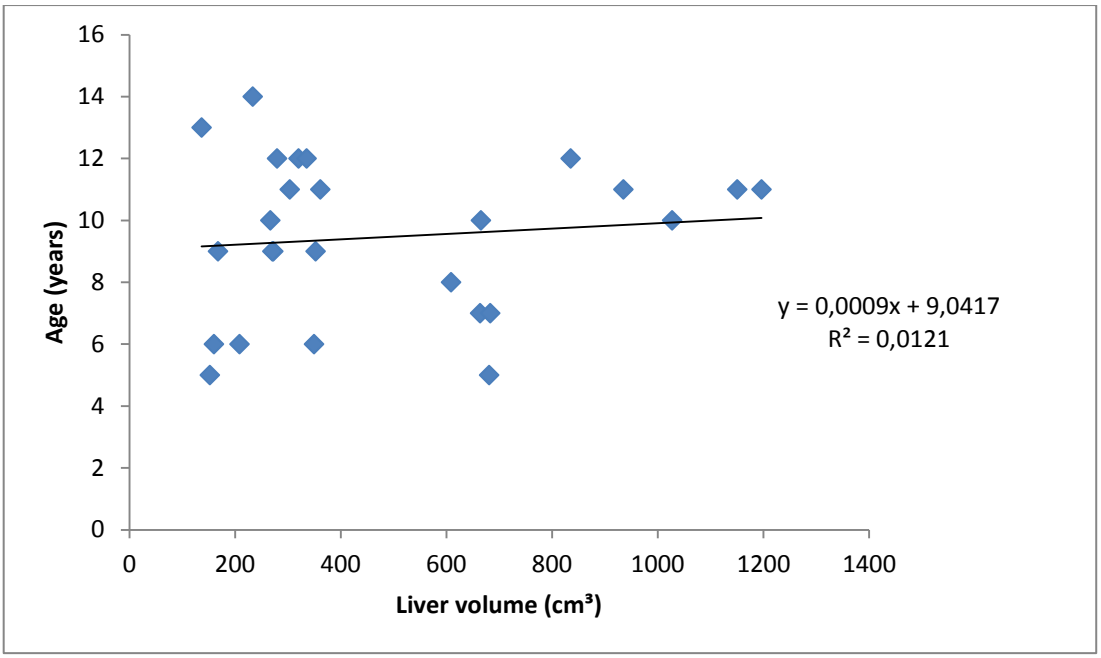

Figure 15. Correlation between liver volume (x-axis) and age (y-axis). The correlation coefficient $R^2 = 0{,}0121$.

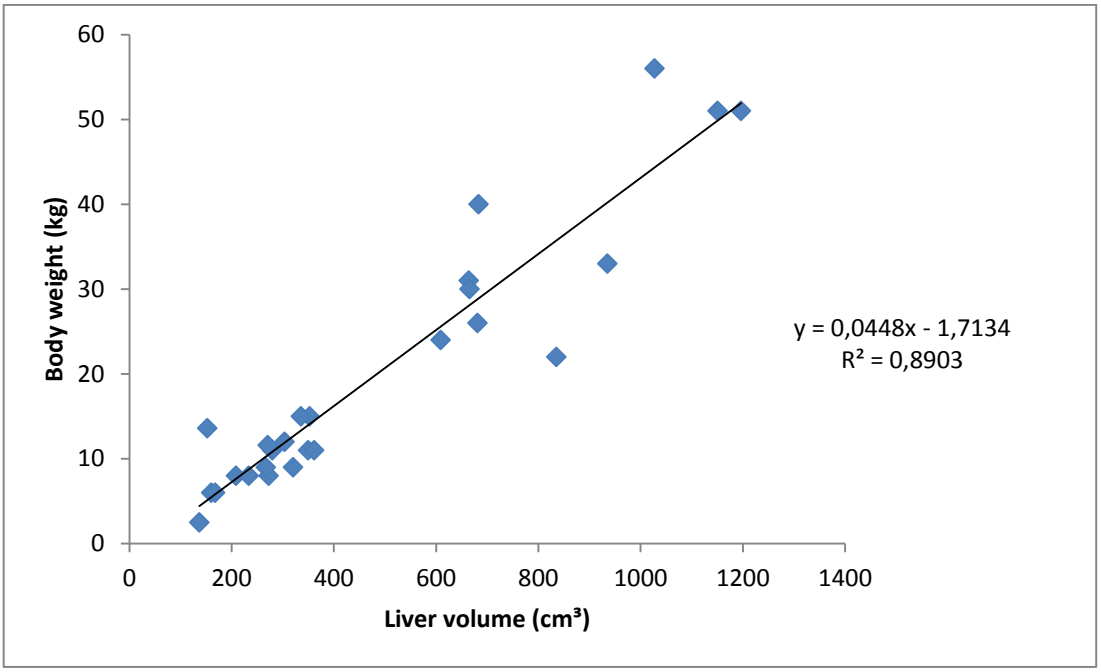

Figure 16. Correlation between liver volume (x-axis) and the body weight (y-axis). The correlation coefficient $R^2 = 0{,}8903$.

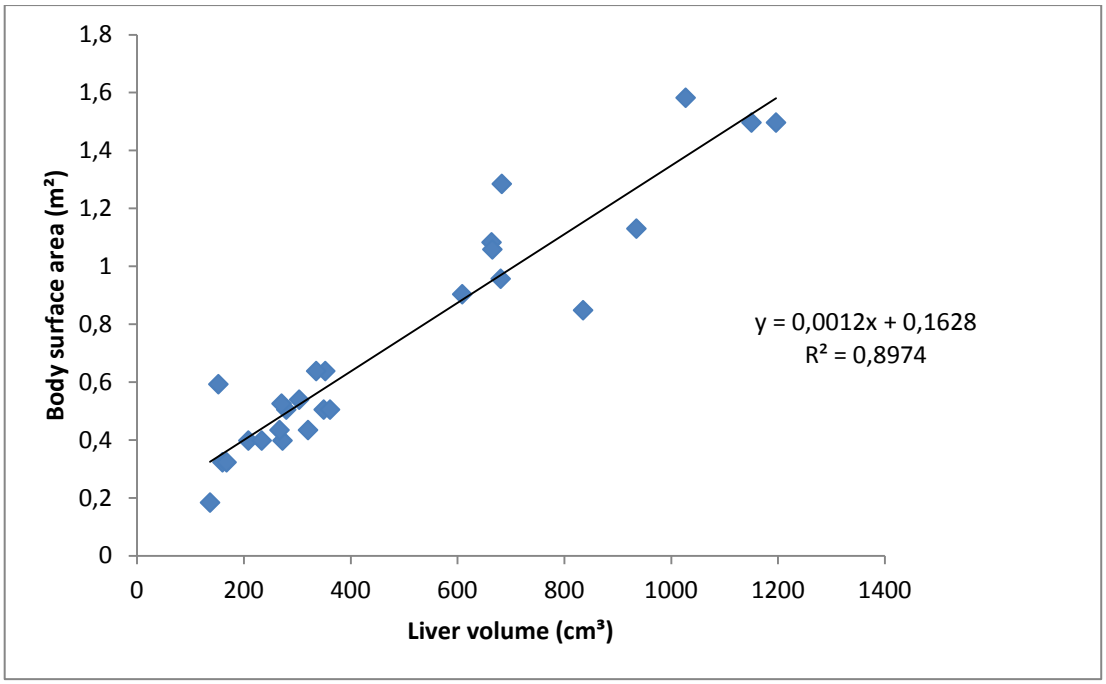

Figure 17. The correlation between liver volume (x-axis) and body surface area (y-axis). The correlation coefficient R^2 = 0,8974.

6. Discussion

This study investigated the relationship between the liver volume of the reconstructed 3D liver obtained manually by 3D Slicer with body variables and several parameters obtained from the analysis of radiographic images.

When assessing liver volume in dogs radiographically, Van Bree et al. stated that liver length, as the distance between the most cranial part of the diaphragm to the apex of the liver tip, is not influenced by thoracic conformation. Therefore, the present study did not take thoracic conformation into consideration when measuring liver length radiographically. Furthermore, Van Bree et al. demonstrated that liver length, taken from radiographic images, correlates well with the liver volume measured by water displacement. These findings were reflected in the results of the present study; as the liver length measured from radiographic images also significantly correlated with liver volume, measured with 3D Slicer. These findings suggest that radiographic liver length is a reliable value for estimating liver volume in dogs. However, on lateral radiographs the ventral and caudoventral borders of the liver were not always clearly visible and therefore, obtaining a precise outline of the liver contours was challenging. In some cases, a merging of liver and spleen was assumed, as similarly described by Douglas and Williamson in their 1970 study.

The liver area, determined from the lateral radiographic images, correlated closely with

liver volume ($p < 0,0001$). As with the liver length values, precise measurements of the area of the liver were made complicated by the outline of the ventral and caudoventral borders of the liver. In addition, the great variability in falciform ligament fat content imposed problems on determining precise liver delineation, especially in obese dogs. This fact was similar to the statement made by Cockett (1986), who described the liver location in obese dogs as holding a more dorsal position while being surrounded by fat depots. Furthermore, Lee and Leowijuk reported that in dogs with an empty stomach it is more difficult to delineate the caudal border of the liver and that in this case, applying a barium meal makes the demarcation between stomach and liver easier to observe. However, in our study no contrast medium was applied to the dogs before imaging.

Godshalk et al. (1990) demonstrated that thoracic width, measured from ventrodorsal radiographic images, correlates with liver volume, measured by water displacement. Similar results were reflected in the present study; as thoracic width, taken from images obtained in dorsal recumbency, also correlated significantly with liver volume, measured with 3D Slicer. The position of the costophrenic recesses on the ventrodorsal radiograph was clearly visible in all 26 patients.

For radiographic assessment of the liver volume, Van Bree et al. calculated the following equation: LL × TD × TW. The results of the formula have shown, similar to the results of our study, a high correlation with liver volume. Moreover, Godshalk et al. stated that the reported body weight of the dogs, correlated with liver volume, determined by water displacement method. In growing dogs, the ratio of liver weight to body weight is higher (O´Brien, 1987), and for this reason no dogs in growing state were included in our study.

In the present study, the body surface area was high statistically significant with liver volume. Similar results were reported from Vauthey et al. (2002) who predicted the liver volume in human adults based on the body surface area. In their radiographic study of liver volume, Godshalk et al. formulated an equation for the calculation of the body surface area in dogs: Body surface area= [(4×body weight)+ 7] /(body weight+90), where body weight is expressed in kilogram and the body surface area in meters squared. In the present study, this formula was used and the results indicated that the calculated body surface area significantly correlated with the liver volume obtained from 3D Slicer. The dogs' age was not statistically significant with the liver volume. It was hereby shown that the age is not a

valid parameter for approaching analysis of the liver volume in dogs. A previous study had shown that gender did not correlate with liver volume, when measured by water displacement (Godshalk et al., 1990). These findings were the reason why the gender of the dog was not taken into consideration in the present study.

One limitation of our study was the inconsideration of breed-dependent variables. Choi et al. stated in their review (2012), that the liver of brachycephalic Pekingese dogs is smaller than the liver of other breeds, indicating a required caution when diagnosing microhepatica in such breeds. Van Bree and Sackx, established radiographic liver size in deep-chested dogs. Even though the dogs were of the same thoracic conformation, a pronounced range in liver size was observed. This physiological variability in hepatic mass, even in dogs with the same thoracic conformation, makes a radiographic assessment of radiological liver size more difficult and a clear observation and diagnosis of a slight hepatomegaly is deemed hardly possible. An additional limitation of our current study was that we could not guarantee that any of the subjects did not harbour a subclinical hepatic disease, as we did not perform any functional tests such as the ammonia tolerance test or peruse any histological examinations. Also, no measurement of the actual liver volume was performed using necropsy and water displacement method by Archimedes principle.

In the current literature regarding radiographic analysis of the liver volume, there is no method which has proven itself to accurately determine the liver size. The radiologists are confronted with discrepancies arising from breed anatomy, thoracic conformation, obesity, and the interference from adjacent organs when visualising the liver borders.
Optimizing radiological technique with regards to the main factors which have been demonstrated to influence liver appearance, namely, breed and thoracic conformation, posture, phase of respiration, obesity, and position of adjacent organs, would aid in radiographic analysis. A comprehensive study in which suitable groups of similar conformational types are categorised to define normal ranges between the breeds would be of use for creating hepatometric criteria for radiographers. Furthermore, a high variability in clinically normal liver size, shape and position, hinders the differentiation between physiological and pathological liver size, especially when discrepancies' are only moderate.
These aforementioned difficulties further support the statement of Douglas and Williamson (1970), who claimed that hepatic survey radiographic images are unreliable in small

animals. For everyday clinical use, this means that there is a high risk of misdiagnosis on the part of the radiologist. Therefore, we could conclude that even if the radiographically evaluated parameters from our study had a statistically significant correlation with liver volume, obtained from 3D Slicer, radiographic analysis is very subjective and offers only a few guidelines for objective evaluations.

CT volume datasets are widely used for quantitative volume analysis. Due to precise organ recognition with cross sectional CT and the ease of scanning these structures in their entirety, CT images potentially offer the most accurate non-invasive method for calculating the liver volume.

Volume reconstruction was based upon an understanding of hepatic anatomy and liver boundaries. The complexity and variability of the liver in its anatomic structures pose many challenging problems for volumetric reconstruction of the liver. Hence, building a liver model is relatively demanding. Diverse training and support resources are available to Users on the 3D Slicer webpage to facilitate the learning process. In recent years, 3D Slicer has gained great recognition in the field of medical imaging research (Fedorov et al., 2012). User interaction was required in each slide to achieve the desired boundary therefore making this method time consuming. In this study, it took 30-45 minutes on average to calculate the liver volume for one patient. Similar results were reported from Lim et al. (2014) in their study, where the average time taken for manual liver segmentation was 39,4 ± 5,5 minutes per case. In contrast, the time for automated volumetry was about 0,57 ± 0,006 minutes per case. In this study, interactive manipulation was done in instances where the required area had been overestimated in the segmentation process, the exceeded volume could be removed with the eraser tool. This liver segmentation method produces satisfactory results in many standard situations, but it might be imprecise in cases where organs with similar grayscale values are adjacent to the liver. This low contrast with regards to neighbouring structures, such as connective tissue and organs such as cardiac muscle or bowel wall, made the segmentation more challenging. The act of scrolling between the slices to get an impression of how the following sequences will appear, gives an overview on how the demarcation between two objects can be determined. In some cases, the grayscale values of the liver are inhomogeneous. This appearance can be either of physiological origin or caused by tumors or metastasis. Furthermore, the enormous variability in the shape of the liver due to high range in natural anatomical structures is quite often difficult to distinguish from pathological circumstances such as cirrhosis, or where a previous surgical intervention has taken place.

A major improvement in computer processing is the availability of reconstruction methods through a simple software which is available for use on personal computers.
The 3D slicer is seen as a valuable software of high potential and abundant clinical relevance both presently and for the foreseeable future.
3D reconstruction allows scientists to create a virtual clone of the patient, which represents a significant value for surgical procedures, especially hepatic surgery. By enabling augmented reality, the patients could benefit from optimisation of the planning and execution of surgical interventions.

Even though there are an array of methods which offer satisfying results in liver volume determination, there is room for improvement in the extraction of a field of interest for further representation through reconstruction. It is, however, assumed that fully automated liver segmentation techniques still produce erroneous segmentations with subsequently serious consequences for the patient (Lim et al., 2014). Therefore, we can conclude that achievement of a timely and precise liver segmentation protocol is an ongoing issue which requires further investigation. With advancing technology, fully automated organ volumetry may replace manual methods for liver volumetric measurements.

7. Abstract

The liver is regarded as one of the most important organs in the body, thus diseases affecting the liver can be potentially fatal. The size and volume of the liver are highly valuable parameters in the diagnosis of hepatic disease processes and are further used as prognostic indicators for preoperative, operative and postoperative considerations.

The aim of this study was to determine if the radiographic assessment of liver size significantly correlates with the real liver volume, as measured by CT volumetry. The study included 26 patients from whom we obtained lateral and ventrodorsal abdominal radiographs and contiguous abdominal CT scans. Through performing manual slice by slice segmentation of the abdominal CT scans, extrapolated to further attain a 3D model reconstruction within the 3D Slicer software, the liver volume was concluded.

Several parameters, including liver length and liver area, were computed from the radiographs in order for comparison and correlation with the determined liver volume, as calculated from the CT scans with 3D Slicer. The age, body weight and body surface area of each individual were also recorded and included in our analysis. All parameters obtained from the radiographic images had a statistically significant correlation with liver volume ($p < 0,05$). Moreover, body weight and body surface area also had a high correlation with liver volume.

With these results in mind, manual volume reconstruction of the liver with 3D Slicer is a reliable method, provided that the operator has an expansive knowledge of hepatic anatomy and its relationship to adjacent organs. However, it should be noted that the manual segmentation process, applied in this study, is highly time consuming and thus not suitable for daily clinical use. Despite a positive relationship occurring between parameters obtained from radiographs and the 3D reconstructed liver volume from 3D Slicer, radiographic assessment of liver volume is an unreliable method due to the numerous influential factors which do not allow, in most cases, a wholly objective assessment.

The body weight and the body surface area are guidelines for the estimation of liver volume, but their value should be considered solely as a tendency auxiliary to additional measurements.

Therefore, we can conclude that achievement of a timely and precise liver segmentation protocol is an ongoing issue which requires further investigation. With sophisticated technology, automated volumetry may replace manual volumetry for precise assessment of liver volume.

8. Acknowledgements

First of all, I would like to thank the Department and Clinic of Surgery and Ophthalmology in the University of Veterinary Medicine, Budapest, for giving me the opportunity to write this thesis, letting me take part in their research and for providing data and radiographic and CT images.

My personal thank goes to Dr. Attila Arany-Tóth as the supervisor of my thesis, who has placed his trust in me and offered his invaluable assistance. I very much appreciate your expert guidance, organisation, effort and patience.

I am particularly grateful for the help given to me by Dr. Andras Lasso, senior engineer and associate director of the laboratory for percutaneous surgery at Queen's University, who is part of the worldwide developer 3D Slicer community. He invested his time in me and shared his expansive knowledge regarding the 3D Slicer.

I would like to express my gratitude to my mum, my dad, my brother and my grandmother, who offered me advice and support throughout writing my thesis, at any time.

Finally, I want to thank Eva Augustin for the shared experience, as well as her help, which was given at any time. I am very grateful.

9. Bibliography

- ACKERMAN N., SILVERMAN S. (1977): Radiographic interpretation: liver enlargement. Modern Veterinary Practice. Vol. 58. 949-954 p.
- BEN-HAIN M., EMRE S., FISHBEIN TM., SHEINER PA., BODIAN CA., KIM-SCHLUGER L., SCHWARTZ ME., MILLER CM. (2001): Critical graft size in adult-to-adult living donor liver transplantation: Impact of the recipient´s disease. Liver Transpl. Vol. 7. No. 11. 948-953 p.
- VAN BREE H., SACKX A. (1987): Evaluation of radiographic liver size in twenty-seven normal deep-chested dogs. Journal of Small Animal Practice. Vol. 28. No. 8. 693-703 p.
- VAN BREE H., VEERLE J., VANDEKERCKHOVE P. (1989): Radiographic assessment of liver volume in dogs. American journal of Veterinary Research. Vol. 50. No. 9. 1613-1615 p.
- CARLSON W.D. (1976): Veterinary Radiology, 2nd edn., pp. 336-342. Lea and Febiger, Philadelphia.
- CHOI J., KEH S., KIM H., KIM J., YOON J. (2012): Radiographic Liver Size In Pekingese Dogs Versus Other Dog Breeds. Veterinary Radiology and Ultrasound. Vol. 54. No. 2. 103-106 p.
- COCKETT P.A. (1986): Radiographic anatomy of the canine liver: simple measurements determined from the lateral radiograph. Journal of Small Animal Practice. Vol. 27. No. 9. 577-589 p.
- DOUGLAS S.W., WILLIAMSON H.D. (1970): Veterinary Radiology Interpretation, pp. 202-2013. Heinemann, London
- FEDOROV A., BEICHEL R., KALPATHY-CRAMER J., FINET J., FILLION-ROBIN J.C., PUJOL S., BAUER C., JENNINGS D., FENNESSY F., SONKA M., BUATTI J., AYLWARD S., MILLER J.V., PIEPER S., KIKINIS R. (2012): 3D Slicer as an image computing platform for the Quantitative Imaging Network. Magnetic Resonance Imaging. Vol. 30. 1323-1341 p.
- GELFAND D.W. (1975): The liver: plain film diagnosis. Seminars in Roentgenology. Vol. 10. No. 3. 177.186 p.
- GIBBS C. (1981): Radiological features of liver diseases in dogs and cats. Veterinary Annual. Vol. 21. 239-249 p.

- GODSHALK C.P., KNELLER S.K., BADERTSCHER R.R., ESSEX-SORLIE D. (1990): American Journal of Veterinary Research. Vol. 51. No. 9. 1421-1426 p.
- GRANDAGE J. (1974): The radiology of the dogs diaphragm. Journal of Small Animal Practice. Vol. 15. 1-17 p.
- GUGLIELMI A., RUZZENENTE A., CONCI S., VALDEGAMBERI A., LACONO C. (2012): How much remnant is enough in liver resection? Dig Surg. Vol. 29. No. 1. 6-17 p.
- VAUTHERY J.N., ABDALLA E.K., DOHERTY D.A., GERTSCH P., FENSTERMACHER M.J., LOYER E.M., LERUT J., MATERNE R., WANG X., ENCARNACION A., HERRON D., MATHEY C., FERRARI G., CHARNSANGAVEJ C., DO K A., DENYS A. (2002): Body Surface Area and Body Weight Predict Total Liver Volume in Western Adults. Liver transplantation. Vol. 8. No. 3. 233-240 p.
- KEALY K. (1979): Diagnostic Radiography of the Dog and the Cat, pp. 19-20. W. B. Saunders and Company, Philadelphia.
- KÖNIG H.E., LIEBICH H.G. (2011): Anatomie der Haussäugetiere. Lehrbuch und Farbatlas für Studium und Praxis. Stuttgart, Schattauer. 355 p.
- LEE R., LEOWIJUK C. (1982): Normal parameters in abdominal radiology of the dog and cat. Journal of Small Animal Practice. Vol. 23. 251-269 p.
- LIM W.C., TAN C.H., CAI J., ZHENG J., KOW W.W.C. (2014): CT volumetry of the liver: Where does it stand in clinical practice. Clinical radiology. Vol. 69. 887-895 p.
- LUSTED L.B., KEATS T.E. (1976): Atlas of Roentgenographic measurements. Vol. 2. Yearbook Medical Publishers, Chicago
- O´BRIEN T.R. (1978): Radiographic Diagnosis of Abdominal Disease in Dog and Cat, pp. 396-480. W.B Saunders and Company, Philadephia.
- PARTINGTON B.P., BILLER D.S. (1995): Hepatic Imaging With Radiology And Ultrasound. Section of Veterinary Radiology. Vol. 25. No. 2. 305-335 p.
- ROOT C.R. (1974): Interpretation of abdominal survey radiographs. Veterinary Clinics of North America. Vol. 12. 153-173 p.
- Introduction - SlicerWeb, 2017. Available from: https: <http://www.slicer.org/pages/Introduction>. (18.03.2017).
- STRAKOS P., JAROS M., KARASEK T., KOZUBEK T., VAVRA P., JONSZTA T.

(2015): Review of the Software Used for 3D Volumetric Reconstruction of the Liver. International Journal of Computer, Control, Quantum and Information Engineering. Vol. 9. No. 2. 369-373 p.

- SUTER P.F. (1982): Radiographic diagnosis of liver disease in dogs and cats. Veterinary Clinics of North America. Vol. 12. 153-173 p.
- TSANG LL., CHEN CL., HUANG TL. (2008): Preoperative imaging evaluation of potential living donors: reasons for exclusion from donation in adult living donor liver transplantation. Transplant Proc. Vol. 40. No. 8. 2460-2462 p.
- WRIGLEY R.H. (1985): Radiographic and ultrasonographic diagnosis of liver disease in dogs and cats. Veterinary Clinics of North America. Vol. 15. No. 1. 21-38 p.